

1 Article Type: Full Paper

2 Quantification of aldehyde terminated heparin by SEC-MALLS-UV
3 for the surface functionalization of polycaprolactone biomaterials

4 Authors: Scott A. Irvine^{†1}, Terry W.J. Steele^{†1,*}, Ramya Bhuthalingam¹, Min Li⁴, Souhir
5 Boujday^{1,2,3}, Melissa Prawirasatya¹, Koon Gee Neoh^{4,5}, Freddy Yin Chiang Boey¹, Subbu S.
6 Venkatraman^{1,*}

7 [†]These authors contributed equally to this manuscript.

8 ¹Nanyang Technological University
9 Materials and Science Engineering
10 Division of Materials Technology
11 N4.1-01-30, 50 Nanyang Ave
12 Singapore 639798

13
14 ² Sorbonne Universités, UPMC Univ Paris 6, UMR CNRS 7197, Laboratoire de Réactivité de
15 Surface, F75005 Paris, France

16 ³ CNRS, UMR 7197, Laboratoire de Réactivité de Surface, F75005 Paris, France

17 ⁴ Department of Chemical and Biomolecular Engineering, National University of Singapore,
18 Kent Ridge, Singapore 117576

19 ⁵ National University Hospital, Kent Ridge, Singapore 117576

20 *Corresponding Authors:

21 Terry W.J. Steele: wjsteele@ntu.edu.sg, (Ph) +65-6790-7594 (Fax) +65-6790-9081

22 Subbu S. Venkatraman: assubbu@ntu.edu.sg, (Ph) +65-6790-4259 (Fax) +65-6790-9081

23 Authors:

24 Scott A. Irvine sairvine@ntu.edu.sg

25 Ramya Bhuthalingam BRamya@ntu.edu.sg

26 Souhir Boujday souhir.boujday@upmc.fr

27 Min Li chelim@nus.edu.sg

28 Melissa Prawirasatya melissa.ps@gmail.com

29 Koon Gee Neoh chenkg@nus.edu.sg

30 Freddy Yin Chiang Boey mycboey@e.ntu.edu.sg

31 Keywords: heparin, aniline, size exclusion chromatography, surface functionalization

32

33

34 **Abstract**

35 A straight forward strategy of heparin surface grafting employs a terminal reactive-aldehyde
36 group introduced through nitrous acid depolymerisation. An advanced method that allows
37 simultaneously monitoring of both heparin molar mass and monomer/aldehyde ratio by size
38 exclusion chromatography, multi-angle laser light scattering and UV-absorbance (SEC-
39 MALLS-UV) has been developed to improve upon heparin surface grafting. Advancements
40 over older methods allow quantitative characterization by direct (aldehyde absorbance) and
41 indirect (Schiff-based absorbance) evaluation of terminal functional aldehydes. The indirect
42 quantitation of functional aldehydes through labeling with aniline (and the formation of a
43 Schiff base) allows independent quantitation of both polymer mass and terminal functional
44 groups with the applicable UV mass extinction coefficients determined. The protocol was
45 subsequently used to synthesize an optimized heparin-aldehyde that had minimal
46 polydispersity ($PDI < 2$) and high reaction yields (yield $> 60\%$ by mass). The 8 kDa weight
47 averaged molar mass heparin-aldehyde was then grafted on polycaprolactone (PCL), a
48 common implant material. This optimized heparin-aldehyde retained its antithrombin activity,
49 assessed in freshly drawn blood or surface immobilized on PCL films. Anticoagulant activity
50 was equal to or better than the 24 kDa unmodified heparin it was fragmented from.

51

52 **Introduction**

53 Haemocompatibility is a major concern in clinical application of devices or biomaterials. The
54 complexity of surface thrombosis of polymeric biomaterials restricts their use in blood
55 environment. Hoffman et al's 1972 manuscript first described the covalent immobilization of
56 heparin to construct a non-thrombogenic surface.[1] After nearly 40 years of research,
57 heparin coating of surfaces still offers one of the best solutions for producing an anti-clotting
58 surface.[2] The tethering of the heparin by a terminal functional group to the polymer (also
59 referred to as end- point attachment) enables better preservation of its functional properties
60 when compared to other techniques involving immobilization at multiple points.[3-5] The
61 single point attachment allows heparin to protrude from the surface and interact with
62 circulating molecules such as antithrombin.

63 Such attachment requires creating a reactive functional group at the terminus of the heparin
64 chain for its subsequent covalent bonding to the surface. One well-recognized approach
65 involves nitrous acid depolymerization to create heparin oligomers with reactive aldehyde
66 groups. This has proven itself in the fabrication of heparin coated biomedical devices, such as
67 the Carmeda® Bioactive Surface coating.[2, 6]

68 Heparin is composed of disaccharides containing L-iduronic acid and D-glucosamine
69 residues [7] as seen in Figure 1. However, heterogeneity exists across the heparin polymer as
70 the disaccharides undergo various chemical modifications producing a range of residues. In
71 particular, 85-90% of D-glucosamine is N-sulphated and the rest are N-acetylated. The
72 various residues react differently to nitrous acid treatment, which necessitates empirical
73 optimization during acid depolymerization. The deamination and subsequent chain cleavage
74 at pH 1.5 is highly specific at N-sulphated D-glucosamine residues whereas at pH 4.5 it is
75 preferential for the unsubstituted D-glucosamine (~ 3% overall) and a minority of N-
76 sulphated (5-8%).[7, 8]

FIGURE 1

77

78 The depolymerization products require monitoring for optimal oligomer chain lengths and
79 MW sizes. If the reaction goes to completion the heparin will be broken down to
80 disaccharides of approximately 1200 Da. However, the minimal effective antithrombogenic

81 unit of heparin consists of a pentasaccharide, where the minimal molecular weight is ~1500
82 to 3000 Da.[9] The pentasaccharide contains the minimum antithrombin sequence sufficient
83 for interacting with and inhibiting Factor Xa, thus preventing thrombogenesis. Monitoring the
84 degree of depolymerization to retain functionality was necessary for correlation to
85 antithrombin activity.[10]

86 A number of methods have been utilized to monitor the resulting molecular weight of the
87 heparin polymer. These include; MALDI-TOF,[11] gel electrophoresis,[12] ¹³C NMR
88 spectroscopy,[13] and intrinsic viscosity.[14] A relatively new method towards characterizing
89 heparin oligomers is size-exclusion chromatography coupled with multi-angle laser light
90 scattering (SEC-MALLS). This provides a rapid, precise and accurate measurement of the
91 molecular weight that does not rely on relative molar mass standards but retains the
92 advantages of HPLC (i.e. automation and productivity). [15-17]

93 For the purpose of end-point immobilization, one also needs to quantitate the presence of the
94 intact aldehyde group after acid depolymerization. The reactive aldehyde becomes a
95 convenient method for subsequent grafting reactions. The aldehyde derivatization has
96 previously been used to study heparin structure and sequence using highly sensitive reagents
97 such as o-(2,3,4,5,6-pentafluorobenzyl)hydroxylamine hydrochloride,[18] 2-
98 aminoacridone,[19] and paranitrophenyl hydrazine.[20] While the above reagents work in
99 limited situations for aldehyde characterization, they are poorly soluble, toxic, and relatively
100 expensive. In contrast, aniline is soluble in both aqueous and organic solvents, has small
101 steric profile, and quickly forms a strongly absorbing UV/vis chromophore at 369 nm that is
102 within the optical window of most organic solvents employed for SEC. Aniline has
103 previously been well characterized in aldehyde-derivatizing Schiff base reactions.[21-23]

104 In this manuscript we describe the use of multi-angle laser light scattering and size exclusion
105 chromatography combined with online UV and refractive index detection (SEC-MALLS-UV)
106 to quantitatively assess the heparin depolymerisation, oligomer mass, polydispersity, reaction
107 yield, and heparin monomer/aldehyde ratios. The method was employed to monitor and
108 optimize heparin depolymerisation to yield an 8 kDa oligomer that retained its antithrombotic
109 activity. The optimized heparin-aldehyde was chemically grafted on polycaprolactone (PCL).
110 Finally, the anticoagulant activity of heparin-aldehyde reductive amination-based surface
111 immobilization was compared against multipoint covalent crosslinking of unmodified heparin.

112

113 **Experimental Section**

114 **Materials**

115 Heparin (sodium salt, ~25 kDa) was purchased from Yantai Dongcheng Biochemicals Co.
116 Ltd (China). Sulphuric acid, sodium nitrite, sodium cyanoborohydride, and HPLC-grade
117 aniline were purchased from Sigma-Aldrich Ltd. Inc. (Singapore). All chemicals and
118 materials were used as received.

119 **Heparin depolymerization by nitrous acid**

120 Heparin depolymerization was carried out at pH 1.5 and pH 4.0 as previously described.[10,
121 24] Briefly, freshly prepared nitrous acid was prepared by mixing in a fume hood 100 mL of
122 0.5 M sulfuric acid (for pH 1.5) or 28.5 mL 0.5M sulfuric acid (for pH 4.0) to a solution of
123 100 mL of 1M sodium nitrite or 71.4 mL of 5.5M sodium nitrite, respectively. Heparin (25
124 mg/mL dissolved in 18.3 MΩ water), a 5 mL aliquot, was added to 20 mL of nitrous acid
125 reagent (pH 1.5 or 4) that was cooled to 0°C or 25°C. Aliquots of 5 mL were taken at 0, 10,
126 20, and 45 min and subsequently neutralized with 1 M sodium hydroxide to yield a final pH
127 of 8.5. Neutralized aliquots were dialyzed (10 kDa MWCO) against 1 L deionized water
128 (diH₂O) for 12 h, with the water replaced every 3 h. Dialyzed samples were lyophilized and
129 stored at 4°C.

130 **Aniline derivatization of Heparin-aldehyde oligomers**

131 Aniline acetate reagent (10 μL of 10% v/v aniline in glacial acetic acid) was added to 90 μL
132 of the depolymerized heparin dissolved at 25 mg/mL lyophilized powder in diH₂O. After 1h
133 at RT, the samples were diluted to 0.5 mL and filtered (0.22 μm) into 1 mL glass HPLC vials
134 for SEC-MALLS-UV (size exclusion chromatography multi-angle laser light scattering-
135 ultraviolet) online characterization or they were subsequently processed for Schiff-base
136 reduction. Reduction of the Schiff-base was performed by adding 50 μL Coupling Buffer (50
137 mM NaBH₃CN in phosphate buffered saline) to the aniline acetate/depolymerized heparin
138 solution described above. The reaction mixture was incubated an additional 1h at RT, diluted
139 to 0.5 mL, filtered in HPLC vials, capped, and then analyzed by SEC-MALLS-UV.

140 **SEC-MALLS-UV quantitation of heparin and depolymerized heparin**

141 An Agilent 1100 series HPLC pump complete with degasser and PLGel aqueous 50 (Polymer
142 Standards Service, Mainz, Germany) in 35°C thermostated oven was connected in-line with
143 an Agilent 1100 UV/Vis detector, Wyatt MiniDawn 3-angle light scattering detector (light
144 scattering calibration through HPLC grade toluene), and an Agilent 1100 refractive index
145 detector. Elution buffer was 100 mM ammonium nitrate with 0.8% w/v sodium azide (pH 7.0)
146 at a flow rate of 1.0 mL/min. Injection volumes were typically 50 μ L. UV Extinction
147 coefficients of aldehyde, phenyl Schiff-bases, and reduced phenyl Schiff-base (phenyl alkyl-
148 amine) were quantified using glutaraldehyde, 1:1 meq ratio of mixed glutaraldehyde:aniline,
149 and reduced glutaraldehyde:aniline, respectively at 280 and 369 nm on cuvette UV/Vis
150 detector. Polymer mass was determined by the refractive index detector using a dn/dc of 0.13
151 for heparin, heparin-Schiff bases, and heparin-phenyl amine using the Wyatt ASTRA
152 (version 5.19.1) software. The slight increase of mass from the aniline conjugation was
153 negligible, but was factored into the dn/dc calculations (which derives the polymer mass)
154 using the 'protein conjugate' template in the Wyatt Astra software. This software factors in
155 the UV/Vis and dn/dc coefficients for both the polymer under analysis and the UV/Vis
156 absorbing conjugate to derive the protein or polymer fraction by weight. Redundant MW
157 analysis was performed by injecting polyethylene glycol standards of known MW to
158 characterize the small molar mass oligosaccharides (< 3 kDa) that had minimal light
159 scattering signals (Polymer Standards Service, Mainz, Germany). M_w and M_n values are
160 generally regarded to be accurate within $\pm 10\%$ on properly calibrated SEC. Quantitation of
161 polymer conjugate values (Table 1), heparin/aldehyde molar ratios, % reaction yield values
162 were performed in triplicate.

163

164 **Heparin surface functionalization of polycaprolactone (PCL)**

165 Approximately 5g of PCL (Polycaprolactone) pellets were pressed into PCL films using a
166 hydraulic hot-press (150 bar), at 70°C for 5 minutes. After cooling, the PCL film was sliced
167 into 5x50 mm strips. The PCL strips were treated with 1N NaOH for 24h at 50°C, then
168 washed with diH₂O and dried at room temperature for 24h. A portion of the alkaline treated
169 PCL was subsequently treated with 40% w/v ethylenediamine/methanol solution for 1h at RT
170 before they were soaked in 4°C PBS for 30 min, rinsed with additional PBS, and then
171 vacuum dried overnight (PCL-NH₂ samples).

172 PCL films with a single point, end-terminal functional group immobilization (PCL-HEP
173 samples) were synthesized with optimized heparin-aldehyde conditions (depolymerization
174 parameters @ pH 4.0, 25°C for 20 min, with 10 kDa MWCO dialysis). PCL-NH₂ strips were
175 immersed in optimized heparin-aldehyde (10 mg/mL) in Coupling Buffer (50 mM NaBH₃CN
176 in phosphate buffered saline) for 2h at RT. Following the reaction, the films were soaked in
177 4°C PBS for 30 min, rinsed with addition PBS, and then vacuum dried overnight (PCL-HEP
178 samples).

179 A control sample of electrostatically bound heparin-aldehyde was adsorbed on to alkaline
180 treated PCL to yield PCL-AHA. Alkaline treated PCL strips were immersed in optimized
181 heparin-aldehyde (10 mg/mL) for 2h at RT and then rinsed with diH₂O. Alternatively,
182 unfractionated heparin (-NH₂ on GlcN disaccharides) was bound covalently to alkaline
183 treated PCL (-COOH groups on PCL surface) through EDC/NHS coupling for a multipoint
184 coupling comparison (PCL-MPH samples). Alkaline treated PCL strips were immersed in 50
185 mM MES buffer (pH 5.6) containing 50 mM EDC and NHS for 10 min at RT, before
186 unfractionated heparin (10 mg/mL) was added. After 2 h, the samples were removed, soaked
187 in 4°C PBS for 30 min, rinsed with additional PBS, and then vacuum dried overnight (PCL-
188 MPH samples).

189 **Thrombogenicity of optimized heparin-aldehyde**

190 Anticoagulant activity of optimized heparin-aldehyde was first qualitatively assessed to
191 ensure anti-thrombosis potential remained after acid depolymerization. Freshly procured
192 Wister rat blood (6 mL, *Rattus norvegicus*) was added to 0.5 mL PBS buffer with the addition
193 of 1) no heparin (neg. control), 2) unfractionated heparin (pos. control), or 3) optimized
194 heparin-aldehyde (both heparin samples at a final conc. of 10 mg/mL) in 15 mL sterile
195 polypropylene tube. Anticoagulant activity was visualized by the darkened red clot within a 6
196 cm petri dish (Figure 5A).

197 For quantitative analysis of solution based heparin activity a time course clotting assay[25,
198 26]. In brief, recalcified sodium citrate treated blood (30 µL) was mixed with 10 µL of either
199 10mg/mL heparin or heparin aldehyde in PBS with 10 µL of PBS alone as a control. The
200 solutions were incubated at 37°C for pre-determined time points (5, 10, 40, 60 min). To finish
201 the reaction, 5 mL of ddH₂O was added to the blood samples and incubated at 37°C for 5 min.
202 The red hemoglobin stain in water was measured at 540nm using a UV-Vis spectrometer.

203 The greater the red colour generated, the lesser the thrombosis, since the released hemoglobin
204 originated from erythrocytes separate from any clotting.

205

206

207 **Anticoagulant and platelet adhesion of surface functionalized PCL strips**

208 Anticoagulant activity of surface functionalized PCL was quantitatively assessed through
209 surface activated clot formation and subsequent color density analysis (ImageJ Densitometry
210 plugin [27]). This assay is based on the material surfaces ability to absorb plasma proteins
211 leading to fibrin formation and erythrocyte adhesion through thrombin activated Factor XIII
212 activity, firstly forming a red gel like coating which may proceed to the darker red clot
213 formation [28, 29], hence the colour intensity and area relate to the anticoagulant properties
214 of the surface. High resolution images were recorded with preset aperture and exposure time.
215 Platelet density from the 64 x 42 μm field of view images could be measured through grey
216 scale density using the image J software, with four separate field of views taken for each film.
217 The PCL strips (in triplicate) were placed in sterile disposable polymethylmethacrylate
218 (PMMA) cuvettes and 1.5 mL of freshly drawn rat blood was quickly added and then covered.
219 Thrombosis was allowed to continue for 30 min at RT, after which the PCL strips were
220 removed and the excess blood was wicked away with Kimwipe tissues. The samples were air
221 dried before photographic analysis. Statistical analysis was performed using t-Test; * = $p <$
222 0.05 and ** = $p <$ 0.01.

223 The *in vitro* thrombo-resistant properties of the PCL samples were determined by kinetic
224 clotting assay similar to that described above. All the testing samples were equilibrated in
225 normal saline water and placed in 12 well tissue culture plates prior to the assay. Fresh
226 sodium citrate treated blood (20 μL) was added onto the sample films and controls (in
227 triplicate) in an open atmosphere. The blood was recalcified with 10 μL of 0.2M CaCl_2 and
228 incubated at 37°C for pre-determined time points (5, 10, 40, 60 min), at which point, 5ml of
229 ddH₂O was added into each well and incubated at 37°C for 5 min. The red stained water was
230 measured at 540nm using a UV-Vis spectrometer.

231

232 Platelet Adhesion was performed as described previously[30]. Briefly, fresh rabbit blood was
233 mixed with 3.8 % (w/v) sodium citrate solution at a dilution ratio of 9:1, respectively. It was

234 then centrifuged at 700 rpm for 10 min to obtain platelet-rich plasma (PRP). The PRP was
235 diluted with PBS in a 1:1 (v/v) ratio. Diluted (PRP 0.1 mL) was then introduced onto 1 sq.
236 cm PCL samples and incubated at 37 °C for 1 h. After incubation, samples were rinsed with
237 PBS and fixed with 3 % (v/v) glutaraldehyde/PBS overnight at 4 °C, and subjected to serial
238 dehydration with 10%, 25%, 50%, 75%, 90% and 100% ethanol for 10 min each. Samples
239 were dried, platinum coated, and observed under scanning electron microscopy . Platelet
240 adhesion was determined by counting the total number of adherent platelets from
241 representative SEM images at the 2000x magnification and normalized to pristine PCL.

242 **X-ray photoelectron spectroscopy of PCL films**

243 To verify the immobilization of the heparin groups on polycaprolactone pristine PCL, PCL-
244 NH₂, and PCL-HEP (optimized heparin-aldehyde conditions at pH 4.0, 25°C for 20 min,
245 with 10 kDa MWCO dialysis grafted onto PCL-NH₂) films were analyzed by X-ray
246 photoelectron spectroscopy (VG ESCA Lab-220i XL XPS) with monochromatic Al K α
247 (1486.71 eV) X-ray radiation (15 kV and 10 mA). The analysis area was 700 x 700 μ m with
248 maximum analysis depth of ~4-8nm. Pass energies of 150 eV and 20 eV were used for the
249 survey scans and high-resolution scans, respectively.

250 **Results**

Figure 1

251

252 **λ_{\max} and UV mass extinction coefficient for aldehyde and Schiff-base quantitation**

253 Heparin was depolymerized in two reaction conditions at pH 1.5 and pH 4.0. The majority of
254 the heparin monomers consist of disaccharides with one of three functional groups; '-H', '-
255 SO₃', or an acetyl group, referred to the monomer abbreviations as GlcN, GlcNSO₃, or
256 GlcNAc, respectively. At pH conditions of 1.5 and 4.0, heparin fragmentation is expected at
257 GlcNSO₃ and GlcN disaccharides, respectively, as illustrated in Figure 1. Initial wavelengths
258 scans of simple alkyl-aldehydes (i.e. glutaraldehyde, butanal) revealed a broad λ_{\max} of 280 nm.
259 We found that this could be used as a qualitative assessment of the aldehyde functional group,
260 but was not ideal for quantitation for number of reasons; 1) Stabilized solvents such THF
261 (w/BHT) have considerable absorbance at wavelengths < 300 nm and 2) direct mass
262 extinction coefficients of aldehyde tend not to be linear, reproducible, or both. For example,

263 when glutaraldehyde was injected as a standard into the SEC-MALLS-UV, it was found to
264 interact with the SEC column materials, resulting in uncharacteristically long elution times (>
265 15 min, data not shown). We proceeded to stabilize the heparin-aldehydes for extinction
266 coefficient linearity and to prevent the terminal aldehydes from interacting with SEC column
267 packing. Aniline was found to be a common laboratory reagent, soluble in both aqueous and
268 organic phases, and has been well characterized towards rapid reactions with simple
269 aldehydes[31]. Under the Schiff-base derivatization procedure, aniline was in high molar
270 excess under acidic conditions, an environment where aldehyde reactions can be safely
271 assumed to be driven to completion. The phenylimine Schiff base possesses a UV mass
272 extinction coefficient ($\lambda_{\text{max}} = 369 \text{ nm}$) that is optimal for SEC analyses--large enough for
273 nanogram sensitivity, but small enough to avoid saturation of the UV signal. This was an
274 important consideration, especially concerning the relatively high amounts (compared to
275 HPLC) of heparin oligomer that was needed for injection, to achieve signal to noise ratios
276 required for quantitative evaluation for the three online detectors (MALLS, UV, and
277 refractive index). For example, injections of 100-1000 μg of oligomer are common for small
278 MW (<20 kDa) characterization by multiangle light scattering and refractive index detectors.
279 Table 1 lists the parameters determined for the calculation of oligosaccharide molar masses
280 and quantitation of the aniline Schiff-base.

Table 1

281

282 **SEC-MALLS-UV characterization of depolymerized heparin and of aldehyde-**
283 **derivatized Schiff bases by aniline.**

284 Figure 1 displays the sequence of reactions, from nitrous acid depolymerization, Schiff-base
285 derivatization with aniline and finally to Schiff base reduction with sodium cyanoborohydride.
286 Figure 2A (refractive index detector, RI) and 2B (UV_{280} absorbance) shows the overlaid
287 SEC-MALLS-UV data of the commercial porcine heparin as well as the depolymerized and
288 fractionated heparin (at two reaction conditions) before Schiff-base derivatization. The
289 reaction conditions were 10 min incubation at 25°C and at pH 1.5 and pH 4.0. The
290 commercial porcine derived heparin had a broad peak, indicative of a large polydispersity,
291 with a weight-averaged molar mass (M_w) of 24 kDa. Acid depolymerization of this sample at
292 pH 1.5 and pH 4.0 had remarkably different SEC profiles. When cleavage occurred at the
293 GlcN disaccharides (at pH 4.0), a dual peak elution profile was present—suggesting only 1-2

294 cleavages in the original porcine heparin polymer as seen in Figure 2A. This dual peak
295 profiles comes about from cleavage near the polymer terminus, generating small molar mass
296 fragments (weight-averaged molar mass, $M_w < 5$ kDa, peak retention volume > 9.5 mL) with
297 a remaining larger molar mass fragment ($M_w > 10$ kDa, peak retention volume < 9.5 mL).
298 At low pH, virtually non-specific cleavage occurs, since the majority of the disaccharides in
299 heparin have the GlcNSO₃ functional group. To remove as much of the smaller fragments as
300 possible, dialysis was performed at 10 kDa molecular weight cutoff, diluting the mono, di,
301 tri-‘disaccharides’ etc. to negligible levels (henceforth ‘fractionated heparin’). This was done
302 to concentrate the higher molecular weight oligomers that remained. While the RI signals,
303 which are a direct measure of sample mass, display ~ 100 μ g of fractionated heparin mass (in
304 Figure 2A), the UV₂₈₀ signal was distinguishable for pH 1.5 fractionated heparin, but barely
305 above the limit of quantitation (signal/noise = ~ 4) for pH 4.0 reaction conditions.

Figure 2

306

307 To demonstrate the improvement in sensitivity, the same fractionated heparin (pH 4.0, 10
308 min. incubation, 25°C depolymerization reaction conditions) and its terminal aldehyde group
309 was derivatized with aniline to yield the phenyl-imine (henceforth Schiff-base). Figure 2C
310 displays the UV₃₆₉ signals of the overlaid heparin-aldehyde (Figure 2C, black line) and the
311 Schiff base (grey line), which was subsequently reduced to the heparin-aniline (dashed black
312 line). For the three overlaid signals, injected mass was ~ 100 μ g, with a representative plot
313 displayed on the right axis (open circles). The UV₃₆₉ AUC (area under curve) signal was
314 increased by over 2 orders of magnitude by converting the terminal aldehyde into the Schiff
315 base. Treatment by sodium cyanoborohydride, a water soluble Schiff base/imine reducing
316 agent, caused the AUC to fall by an order of magnitude. This provided sufficient evidence
317 that the aldehyde was present, converted to Schiff base, and then subsequently reduced to the
318 phenylaniline.

319 **Optimized heparin-aldehyde M_w is prepared at pH 4.0, 25°C, and 20 min reaction time**

Figure 3

320

321 The molar mass from the pH 1.5 depolymerized and fractionated heparin oligomers never
322 exceeded 4 kDa as seen in Figure 3A. The quantitation of the aldehydes was compared to the
323 molar amount of disaccharides present in heparin, since this is the smallest repeating unit or
324 ‘monomer’ in heparin. In Figure 3A, the right axis displays the molar ratio of heparin
325 disaccharides/aldehyde (always present on the terminal depolymerized heparin). If the
326 heparin was completely depolymerized into its disaccharide building blocks, the ideal ratio
327 would be 1:1. The molar mass differences were negligible in the nitrous acid incubation
328 conditions of 10 or 20 minutes at either temperature tested. After 45 minutes in pH 1.5,
329 regardless of temperature, no oligomer elution peaks were seen by the SEC
330 characterization—the heparin had been completely depolymerized at this time point, and was
331 diluted to negligible levels in the dialysis cleanup procedure. Taking the average of the four
332 remaining conditions at pH 1.5, ~ 6 heparin disaccharide repeat units were intact per
333 aldehyde terminus after depolymerization and dialysis.

334 The depolymerization at pH 4.0 allowed a milder cleavage mechanism, due to the scarcity of
335 the disaccharides with the GlcN functional group. Lower temperatures and shorter
336 incubations were thus more effective at controlling both molar mass and heparin/aldehyde
337 ratios, as seen in Figure 3B. At 0°C, there was a retarded cleavage rate across the different
338 incubation times, which eventually reached the same molar mass as the 25°C incubation—
339 where cleavage was complete in 10 min or less. Here, weight-averaged molar mass (M_w)
340 could be controlled by temperature and incubation time in the range of 14-20 kDa, although
341 with substantial polydispersity. After 45 min for either temperature, the average
342 heparin/aldehyde ratio was ~12. Polydispersity diminished at 0°C, but no changes were seen
343 from 20 to 45 min at 25°C. Assuming that each disaccharide (on average) has a molar mass
344 of ~ 570 Da, the aldehyde-derivatized heparin molar mass is ~8 kDa. This number agreed
345 well with the number-averaged molar mass (M_n) of 7.5 kDa. Overall, in terms of optimal M_w ,
346 polydispersity, throughput, and reaction yield (see below), the best reactions conditions for
347 heparin-aldehyde were at pH 4.0, 20 min reaction time at 25°C (henceforth ‘optimized
348 heparin-aldehyde’). This optimized heparin-aldehyde will be the formulation considered
349 towards the subsequent surface functionalization of PCL (PCL-AHA and PCL-HEP samples
350 discussed below) and assessment of blood coagulation.

351 **Reaction yields of depolymerized heparin followed by dialysis**

352 After the heparin depolymerization, dialysis was employed to remove the smallest fragments
353 and selectively concentrate the largest oligosaccharides. This had the desired effect, but at a
354 cost of losing a percentage of the original heparin. Figure 3C compares the reaction yields of
355 the twelve different reaction conditions. With the largest amount of cleavage attained at pH
356 1.5, a majority of the heparin was converted into fragments less than 2 kDa and dialyzed
357 away due to the 10 kDa molecular weight cutoff (MWCO) dialysis membrane. As such, only
358 ~25% of the original heparin remained at 10 and 20 min. An increased reaction yield was
359 seen for the pH 4.0 reactions, where ~60% of the original heparin was retained. No
360 statistical difference in reaction yields were seen between the 0°C and 25°C under the same
361 pH conditions.

362 **Surface functionalization of PCL strips with optimized heparin-aldehyde**

Figure 4

363

364 The PCL strips underwent alkali treatment and aminolysis to introduce surface primary amine
365 groups, as depicted in Figure 4. No significant differences were found for the PCL M_w after
366 alkali treatment (data not shown). X-ray photoelectron spectroscopy (XPS) characterized
367 presence of amine groups and the subsequent grafting of optimized heparin-aldehyde. XP
368 spectra of C1s, O1s, N1s, and S2p are shown in Figure 4 and the data summarized in Table 2.
369 As expected of organic polymer films, all survey spectra displayed carbon and oxygen in
370 various ratios. C1s spectra show three contributions, C-C, C-O, and C=O at ~285, 287, and
371 289 eV, respectively.[32, 33] The O1s spectra, also shown in Figure 4, were fitted
372 considering three contributions: at 532.2 and 533.7 eV, attributed to C=O and C-O,
373 respectively and the third at 531.3 attributed to oxygen species in sulfates groups. Upon
374 heparin grafting an intense peak of sulfur was recorded, suggesting the successful grafting or
375 adsorption of heparin-aldehyde on the PCL-HEP sample. Simultaneously, the O1s
376 contribution at 531.3 eV rising from oxygen species in sulfates groups increased consistently
377 with S2p peak increase. The integration of the doublet 2p_{3/2} and 2p_{1/2} at 168.7 and 170 eV,
378 respectively, allowed us to quantify 0.6% S on the surface. In contrast, only traces of sulfur,
379 possibly arising from sulfates contamination, were detected on the PCL-NH₂ strips.

380 Nitrogen/carbon (N/C), determined from both contributions in N1s peak (-NH₂ and -NH₃⁺, at
381 399.8 and 401.6 eV, respectively) and oxygen/carbon (O/C) ratios also increased as a
382 consequence of heparin-aldehyde grafting. For both the PCL-NH₂ samples and PCL-HEP

383 samples, traces of sodium and chlorine were present, likely due to the phosphate buffered
384 saline rinses (data not shown).

Table 2

385

386 The molecular formula of a Heparin disaccharide is $C_{12}H_{19}NO_{20}S_3$. With the
387 depolymerization described in Figure 1, complete fragmentation at pH 1.5 would yield the
388 disaccharide $C_{12}H_{17}O_{18}S_2$. Therefore, the ratio O/S in the immobilized depolymerized heparin
389 will range between 7 and 9, depending on the degree of depolymerization. Based on this
390 reasoning, we calculated the % of oxygen arising from heparin in Table 2. O/C ratio in PCL
391 is ca. 0.30 and 0.31 in the PCL-NH₂ samples. We calculated O/C ratio for PCL-HEP by
392 subtracting O elements likely arising from heparin. The results were consistent with the
393 expected data (0.30-0.32) indicating that the overall molecular formula of heparin was
394 preserved on the PCL-HEP strips.

395

396 **Blood compatibility of PCL and surface functionalized heparin-aldehyde**

Figure 5

397

398 Qualitatively the heparin aldehyde was initially demonstrated to have noticeable
399 anticoagulant activity, similar to that of unmodified heparin when added to freshly drawn
400 blood, both of which considerably reduced clot formation after 30mins (Figure 5A image).

401 Quantitatively the colorimetric solution based clotting assay (Figure 5A graph) shows that
402 both heparin and heparin aldehyde prevent blood coagulation to a similar degree for the entire
403 60 minute time course.

404 Pristine polycaprolactone (PCL) was subsequently modified by alkaline treatment (PCL-Alk),
405 then with unmodified heparin through electrostatic adsorption (PCL-PeHEP) covalent bound
406 through multipoint amide crosslinking (PCL-MPH) and optimized heparin-aldehyde through
407 nonspecific electrostatic adsorption (PCL-AHA) or through a rapid end-terminal, single point
408 attachment with the aid of a reductive 'Coupling Buffer' (PCL-HEP). The samples were
409 tested over a 60 min time course also using the modified assay (Figure 5B)[25]. The pristine

410 PCL showed good early blood contacting qualities up to 40 mins, possibly due to the relative
411 hydrophobicity of the surface. In comparison PCL-Alk being the most hydrophilic
412 demonstrated the most prothrombotic profile. PCL-MPH, PCL-PeHEP and PCL-AHA all
413 displayed antithrombotic qualities better than the PCL-Alk for the first 40mins. PCL-AHA
414 provided a better surface than either PCL-PeHEP and PCL AHA even though increasing
415 blood clotting was recorded for each of these treatments. However, the PCL-HEP produced
416 the best antithrombotic surface, remaining consistent throughout the experiment with no
417 indication of blood clotting for the entire 60 mins (Figure 5B)

418 A second experiment to assess surface antithrombotic activity by colormetric assessment of
419 surface blood clotting was performed on samples PCL, PCL-MPH, PCL-AHA and PCL-HEP.
420 These samples were immersed in freshly drawn recalcified citrated blood for 30 min, before
421 surface initiated clot formation was assessed.[34, 35] PMMA cuvettes were chosen as the
422 material has a long partial thromboplastin time and have been used to fabricate test cells for
423 blood compatibility assay. The recalcified citrated blood did not clot on the surface of the
424 PMMA cuvettes, instead the clots were generated from the surface of the PCL films in each
425 sample. Results and representative surface clot photographs are displayed in Figure 5C.
426 Unmodified heparin (PCL-MPH) displayed blood clotting density similar to pristine PCL.
427 PCL surface functionalized with optimized heparin-aldehyde (PCL-AHA & PCL-HEP strips)
428 exhibited an order of magnitude less clotting density compared to immobilized unmodified
429 heparin. There was no significant difference in the method of surface immobilization--both
430 had similar low magnitudes of clotting initiation and thrombus density. However, visual
431 inspection of the photographs display that more intermittent clotting densities exist on the
432 PCL-AHA (electrostatically bound) samples than on the PCL-HEP samples. As seen above,
433 this suggests that PCL-AHA samples lacked complete surface coverage or the heparin-
434 aldehyde became competitively displaced over time, as would be expected of nonspecifically
435 bound heparin in a complex blood milieu. In contrast, the PCL-HEP samples displayed the
436 lowest magnitude of thrombus density and had the most visually transparent surfaces. For
437 comparison, the simplified surface chemistries of PCL, PCL-MPH, PCL-AHA, and PCL-
438 HEP are displayed in Figure 5D.

Figure 6

439

440

441 Platelet adhesion and biomaterial surface activation is one of the primary initiating
442 mechanisms of thrombosis.[36, 37] Figure 6A displays the SEM images of adherent platelets
443 on pristine PCL and various heparin modified PCL surfaces. Pristine PCL surfaces are
444 heavily concentrated with adhered, activated platelets, as revealed by their irregular shape
445 and presence of numerous pseudopodia. The surface concentration of adhered platelets is
446 much lower when heparin is carbodiimide-mediated covalently crosslinked to PCL (PCL-
447 MPH). Electrostatically bound (optimized) heparin-aldehyde (PCL-AHA) displays similar
448 activation as seen on pristine PCL (no statistical difference observed), likely due to the
449 inflammatory action of aldehyde functional groups[38]. Compared to PCL, the surface
450 concentration of adhered platelets was halved on heparin-aldehyde that is end-terminal
451 crosslinked to PCL through reductive amination (PCL-HEP). A noticeable proportion of
452 platelets are rounded (unactivated) in the PCL-HEP samples as compared to PCL and PCL-
453 AHA films. As seen in Fig. 6B, PCL-HEP has significantly less platelet adhesion than both
454 PCL and PCL-AHA.

455 **Discussion**

456 The use of static light scattering combined with size exclusion chromatography has been
457 described as the method of choice for determining heparin molecular weight in the absence of
458 a structurally similar calibrant[39, 40]. Since static light scattering molar mass measurement
459 is absolute, this method eliminates the need for calibration using molar mass standards, a
460 considerable advantage when working with chemically unique polymers, as structurally
461 similar standards are usually lacking. Other scenarios require absolute molar mass
462 measurement, especially when polymer-column adsorption interactions are likely (e.g.
463 aldehyde and ketone functional groups).[41-43]

464 A qualitative analysis at UV₂₈₀ allows direct detection of aldehydes, which may be beneficial
465 for separation and fractionation of heparin-aldehyde oligomers. A more sensitive quantitative
466 analysis employing aniline ensures effective quality control of the heparin prior to surface
467 functionalization. The quantitative analysis allows characterization of end-group functionality,
468 aldehyde/molar mass distribution ratios, assessment of side reactions, and heparin-aldehyde
469 half-life determination in various environments. Besides increasing sensitivity, other benefits
470 are noted, including long-term stabilization of the UV chromophore and preventing
471 aldehyde/SEC column interactions. The methodology also allows pre- and post-reduction
472 comparisons, each with unique UV absorbance spectra (phenylimine vs. phenylamine) to
473 quantify the aldehyde content, which may be useful for the reductive coupling of aldehyde-
474 amine functional groups.[44] Heparin fragmentation at pH 4 reaction conditions displayed
475 sufficient reactive aldehyde groups for use in surface immobilization with a molar ratio of
476 aldehyde to disaccharide heparin monomers of 12:1, whereas at pH 1.5 the ratio was greatly
477 reduced to approximately 6:1, after dialysis cleanup. By selective tuning of reaction
478 conditions combined with the proper choice of dialysis membranes, extended ranges of 1:1 to
479 20:1 heparin-aldehyde ratios could be envisioned. The height of the heparin brush border can
480 thus be regulated since a dodecasaccharide (12 mer or 6-disaccharides) has a length of 5 nm.
481 The antithrombotic properties of the heparin decreases with the shortening of the polymer
482 down to the pentasaccharide, for example, by reducing the chain to less than 18
483 oligosaccharides ($M_w = 5400$), antifactor IIa activity becomes undetectable [45].

484 Under optimized reaction conditions (pH 4, 25°C in 20 min or less), optimal molar masses of
485 ~8 kDa heparin (or less) were produced after dialysis. With cleavage of most GlcN residues,
486 no further MW degradation was seen after 20 min. The resultant MW of approximately 8

487 kDa M_w is large enough to have a high probability of including the pentasaccharide sequence
488 responsible for binding antithrombin (approx. 1.5 to 3kDa) [9]. Heparin oligomers of 5 kDa
489 have previously been shown to incorporate anticoagulant active pentasaccharide in 15 to 25%
490 of the fragmented heparin oligomers.[46] Indeed, the optimized heparin-aldehyde (PCL-HEP)
491 described above demonstrated superior whole blood, anticoagulant properties compared to a
492 multipoint attached unmodified heparin (PCL-MPH, Fig. 5B and C) A higher platelet
493 activation is observed due to the likely presence of unreacted aldehyde groups, The inhibition
494 of platelet binding is a property associated with heparin ⁴, however it is not as directly linked
495 to heparin as antithrombotic activity since antithrombosis has been observed without a
496 proportional inhibition of platelet binding[47].The successful Carmeda bioactive surface was
497 developed from studies carried out on surface tethering 8 kDa acid depolymerized heparin,
498 then assessing its antithrombin activity.[48-51] Under optimized reaction conditions, we
499 synthesized an 8 kDa heparin fragment in good yield under mild ambient conditions (aka
500 optimized heparin-aldehyde). Prevention of blood clotting by the optimized heparin-
501 aldehyde compared favorably to unmodified heparin when incubated in freshly drawn rat
502 blood. Surface functionalized heparin, either through electrostatic adsorption or through
503 covalent crosslinking yielded very different anticoagulation activity, when the optimized
504 heparin-aldehyde (8 kDa, PCL-AHA or PCL-HEP samples) was compared to unmodified
505 heparin (24 kDa, PCL-MPH samples). The 8 kDa heparin displayed an order of magnitude
506 less blood clot density which was easily visually discerned in the photographs and
507 statistically significant ($p < 0.01$, Figure 5C). However, no statistical significance was seen
508 between heparin electrostatically or covalently bound to alkaline treated PCL. The XPS
509 spectra showed the presence of heparin which suggests that the strategy of covalent binding
510 succeeded explaining the relatively high anticoagulant activity observed. However, PCL-
511 HEP samples displayed higher platelet activation than PCL-MPH, but less than PCL-AHA,
512 suggesting that inflammatory aldehyde groups are still present after the reductive amination
513 and the method of amination may need further improvement, and will be a focus of our future
514 work. It was unexpected that optimized heparin-aldehyde had considerable amounts of
515 electrostatic binding, as most of the cationic primary amines within the GlcN residues should
516 have converted to terminal aldehyde groups under the acidic depolymerization reactions. We
517 speculate that PCL-AHA still has a fair amount of electrostatic binding through electrical
518 double layer interactions; heparin-aldehyde forms reversible hemiacetal linkages with the
519 available hydroxyl linkages next to acidic carboxylic acids, or combination thereof. Similar
520 aldehyde formation and subsequent hemiacetal formation has been observed in other

521 polysaccharide oxidations.[52, 53] Indeed, a more sophisticated investigation of blood
522 proteins binding to a heparin functionalized surfaces favors hemiacetal formation as well, as
523 it would still have an end-point covalent attachment. Gore et al. concluded that end point
524 attachment of heparin yielded lower coagulation marker than any heparin that was bound by
525 multipoint attachment.[54] Both mechanisms, however, would account for the slow release
526 of heparin from physically adsorbed surfaces.[55, 56]

527 Some of the limitations in this work include assumptions in the stability and equilibrium of
528 the aniline derived Schiff-base (see Figure 1). Although this equilibrium reaction has been
529 known to strongly favor the reaction products, this may change under different conditions of
530 pH, temperature, and buffer.[21-23] However, under the SEC buffer eluent, where there is
531 no excess aniline and the reversible reaction may form small amounts of reactants if the
532 elution times are large. Quantitating these small reactants isn't feasible, as additional
533 chromophores can cause transimination reactions.[57] This reversibility may be an asset if
534 the recovery of the heparin-aldehyde is necessary through the competitive addition of a small
535 and volatile aldehyde (e.g. formaldehyde, acetaldehyde) that removes the aniline. Although
536 this is mentioned for the reader's consideration, the Schiff base is regarded as stabile under
537 ambient physiological conditions. Also, it should be noted that optimized heparin-aldehyde
538 presented throughout this manuscript was only optimized with respect to oligomer synthesis
539 and was not optimized with respect to antithrombin activity, surface concentration, or method
540 of surface functionalization, although many efforts by others have focused on these important
541 areas.[58, 59] With the development of the previously described heparin-aldehyde
542 quantitation assay, our future work will be focused on SEC-MALLS-UV based methods of
543 characterizing heparin immobilized on PCL biomaterials, their mechanisms of binding, and
544 residual amounts of aldehyde functional groups remaining.

545

546 **Conclusion**

547 Herein we have described a method to quantitate the formation of aldehyde-terminated
548 heparin for use in the surface functionalization of biomedical devices. SEC-MALLS-UV
549 based protocol facilitates assay development by detection of Schiff base on the terminal
550 heparin-aldehyde functional group. The online analysis with light scattering, refractive index
551 and UV detectors allows molar mass, concentrations of polymer and aldehyde containing

552 analytes to be quantified independently, simultaneously. The protocol was subsequently used
553 to synthesize an optimized heparin-aldehyde that had minimal polydispersity, high reaction
554 yield and retained antithrombin activity that was equal to or better than the unmodified
555 heparin it was synthesized from.

556 **Acknowledgements**

557 This research is supported by the Singapore National Research Foundation under CREATE
558 programme: The Regenerative Medicine Initiative in Cardiac Restoration Therapy (NRF-
559 Technion). This research was also supported by the Ministry of Education: Tier 1 Grants
560 RG46/11, and RG54/13, and Tier 2 Grant: MOE2012-T2-2-046. TS and SB would like to
561 acknowledge Tan Chin Tuan Fellowship for additional funding. We would like to thank Prof.
562 Peter Preiser and Ximei Huang for their kind assistance.

563

564 **References:**

- 565 [1] A.S. Hoffman, G. Schmer, C. Harris, W.G. Kraft, Covalent binding of biomolecules to radiation-
566 grafted hydrogels on inert polymer surfaces, *Trans Am Soc Artif Intern Organs*, 18 (1972) 10-18.
- 567 [2] S. Venkatraman, X. Yun, H. Yingying, D. Mondal, L.K. Lin, *Bioactive Coatings for Implanted Devices*,
568 in: S. Zhang (Ed.) *Biological and Biomedical Coatings Handbook*
- 569 CRC press2010, pp. 471–489.
- 570 [3] R. Larsson, O. Larm, P. Olsson, The search for thromboresistance using immobilized heparin, *Ann*
571 *N Y Acad Sci*, 516 (1987) 102-115.
- 572 [4] S. Murugesan, J. Xie, R.J. Linhardt, Immobilization of heparin: approaches and applications, *Curr*
573 *Top Med Chem*, 8 (2008) 80-100.
- 574 [5] P. Olsson, J. Sanchez, T.E. Mollnes, J. Riesenfeld, On the blood compatibility of end-point
575 immobilized heparin, *J Biomater Sci Polym Ed*, 11 (2000) 1261-1273.
- 576 [6] N. Stenach, R.L. Korn, C.A. Fisher, V. Jeevanandam, V.P. Addonizio, The effects of heparin bound
577 surface modification (Carmeda Bioactive Surface) on human platelet alterations during simulated
578 extracorporeal circulation, *J Extra Corpor Technol*, 24 (1992) 97-102.
- 579 [7] M.J. Bienkowski, H.E. Conrad, Oligosaccharides formed by treatment of heparin with nitrous acid,
580 *Semin Thromb Hemost*, 11 (1985) 86-88.
- 581 [8] J. Riesenfeld, L. Roden, Quantitative analysis of N-sulfated, N-acetylated, and unsubstituted
582 glucosamine amino groups in heparin and related polysaccharides, *Anal Biochem*, 188 (1990) 383-
583 389.
- 584 [9] Y. Xu, S. Masuko, M. Takeddin, H. Xu, R. Liu, J. Jing, S.A. Mousa, R.J. Linhardt, J. Liu,
585 Chemoenzymatic synthesis of homogeneous ultralow molecular weight heparins, *Science*, 334 (2011)
586 498-501.
- 587 [10] J.S. Turner, M.V. Sefton, Immobilization of a lysine-terminated heparin to polyvinyl alcohol, *J*
588 *Biomater Sci Polym Ed*, 5 (1994) 353-369.
- 589 [11] L. Bultel, M. Landoni, E. Grand, A.S. Couto, J. Kovensky, UV-MALDI-TOF mass spectrometry
590 analysis of heparin oligosaccharides obtained by nitrous acid controlled degradation and high
591 performance anion exchange chromatography, *J Am Soc Mass Spectrom*, 21 (2010) 178-190.
- 592 [12] G.H. Barlow, The determination of molecular weight distributions on heparin samples, *Semin*
593 *Thromb Hemost*, 11 (1985) 26-28.
- 594 [13] U.R. Desai, R.J. Linhardt, Molecular weight of heparin using ¹³C nuclear magnetic resonance
595 spectroscopy, *J Pharm Sci*, 84 (1995) 212-215.
- 596 [14] S.E. Lasker, S.S. Stivala, Physicochemical studies of fractionated bovine heparin. I. Some dilute
597 solution properties, *Arch Biochem Biophys*, 115 (1966) 360-372.
- 598 [15] J.E. Knobloch, P.N. Shaklee, Absolute molecular weight distribution of low-molecular-weight
599 heparins by size-exclusion chromatography with multiangle laser light scattering detection, *Anal*
600 *Biochem*, 245 (1997) 231-241.
- 601 [16] C.D. Sommers, H. Ye, R.E. Kolinski, M. Nasr, L.F. Buhse, A. Al-Hakim, D.A. Keire, Characterization
602 of currently marketed heparin products: analysis of molecular weight and heparinase-I digest
603 patterns, *Anal Bioanal Chem*, 401 (2011) 2445-2454.
- 604 [17] J. Beirne, H. Truchan, L. Rao, Development and qualification of a size exclusion chromatography
605 coupled with multiangle light scattering method for molecular weight determination of
606 unfractionated heparin, *Anal Bioanal Chem*, 399 (2011) 717-725.
- 607 [18] C. Deng, X. Zhang, A simple, rapid and sensitive method for determination of aldehydes in
608 human blood by gas chromatography/mass spectrometry and solid-phase microextraction with on-
609 fiber derivatization, *Rapid Commun Mass Spectrom*, 18 (2004) 1715-1720.
- 610 [19] M. Viola, D. Vigetti, E. Karousou, B. Bartolini, A. Genasetti, M. Rizzi, M. Clerici, F. Pallotti, G. De
611 Luca, A. Passi, New electrophoretic and chromatographic techniques for analysis of heparin and
612 heparan sulfate, *Electrophoresis*, 29 (2008) 3168-3174.

613 [20] Y. Kariya, J. Herrmann, K. Suzuki, T. Isomura, M. Ishihara, Disaccharide analysis of heparin and
614 heparan sulfate using deaminative cleavage with nitrous acid and subsequent labeling with
615 paranitrophenyl hydrazine, *J Biochem*, 123 (1998) 240-246.

616 [21] J.J. Charette, H.E. De, Physicochemical properties of Schiff bases. 4. Tautomeric equilibrium and
617 kinetics of hydrolysis of N-benzylideneaniline derivatives, *J. Org. Chem.*, 44 (1979) 2256-2262.

618 [22] J. Csaszar, J. Balog, Spectra of aromatic Schiff bases, *Acta Chim. Acad. Sci. Hung.*, 86 (1975) 100-
619 116.

620 [23] R.M.D. Del, O.O.D. De, M. Urquia, C. Scarabino, R.A. Yunes, The reaction of aniline with 5-nitro-
621 2-furaldehyde. A model for non-enzymic browning reactions, *Aust. J. Chem.*, 33 (1980) 519-525.

622 [24] H.E. Conrad, Degradation of heparan sulfate by nitrous acid, *Methods Mol Biol*, 171 (2001) 347-
623 351.

624 [25] Y. Imai, Y. Nose, A new method for evaluation of antithrombogenicity of materials, *Journal of*
625 *Biomedical Materials Research*, 6 (1972) 165-172.

626 [26] Y.L. Zhao, S.G. Wang, Q.S. Guo, M.W. Shen, X.Y. Shi, Hemocompatibility of electrospun
627 halloysite nanotube- and carbon nanotube-doped composite poly(lactic-co-glycolic acid) nanofibers,
628 *J Appl Polym Sci*, 127 (2013) 4825-4832.

629 [27] C.A. Schneider, W.S. Rasband, K.W. Eliceiri, NIH Image to ImageJ: 25 years of image analysis, *Nat*
630 *Meth*, 9 (2012) 671-675.

631 [28] A. Bantjes, Clotting Phenomena at the Blood-Polymer Interface and Development of Blood
632 Compatible Polymeric Surfaces, *Brit Polym J*, 10 (1978) 267-274.

633 [29] A. de Mel, B.G. Cousins, A.M. Seifalian, Surface modification of biomaterials: a quest for blood
634 compatibility, *International journal of biomaterials*, 2012 (2012) 707863.

635 [30] M. Li, K.G. Neoh, L.Q. Xu, R. Wang, E.T. Kang, T. Lau, D.P. Olszyna, E. Chiong, Surface
636 Modification of Silicone for Biomedical Applications Requiring Long-Term Antibacterial, Antifouling,
637 and Hemocompatible Properties, *Langmuir*, 28 (2012) 16408-16422.

638 [31] H. Puchtler, S.N. Meloan, On Schiff's bases and aldehyde-fuchsin: a review from H. Schiff to R. D.
639 Lillie, *Histochemistry*, 72 (1981) 321-332.

640 [32] J. Matthew, Surface analysis by Auger and x-ray photoelectron spectroscopy. D. Briggs and J. T.
641 Grant (eds). IMPublications, Chichester, UK and SurfaceSpectra, Manchester, UK, 2003. 900 pp., ISBN
642 1-901019-04-7, 900 pp, *Surf Interface Anal*, 36 (2004) 1647-1647.

643 [33] V.T. Mogal, C.S. Yin, R. O'Rorke, S. Boujday, C. Methivier, S.S. Venkatraman, T.W. Steele, Tuning
644 model drug release and soft-tissue bioadhesion of polyester films by plasma post-treatment, *ACS*
645 *applied materials & interfaces*, 6 (2014) 5749-5758.

646 [34] S.W. Kim, H. Jacobs, Design of nonthrombogenic polymer surfaces for blood-contacting medical
647 devices, *Blood Purificat*, 14 (1996) 357-372.

648 [35] N. Borenstein, J.L. Brash, Red-Blood-Cells Deposit Membrane-Components on Contacting
649 Surfaces, *J Biomed Mater Res*, 20 (1986) 723-730.

650 [36] Y.L. Li, K.G. Neoh, E.T. Kang, Poly(vinyl alcohol) hydrogel fixation on poly(ethylene terephthalate)
651 surface for biomedical application, *Polymer*, 45 (2004) 8779-8789.

652 [37] N. Morimoto, A. Watanabe, Y. Iwasaki, K. Akiyoshi, K. Ishihara, Nano-scale surface modification
653 of a segmented polyurethane with a phospholipid polymer, *Biomaterials*, 25 (2004) 5353-5361.

654 [38] V. Schmidt, T. Hilberg, G. Franke, D. Glaser, H.H.W. Gabriel, Paraformaldehyde fixation induces a
655 systematic activation of platelets, *Platelets*, 14 (2003) 287-294.

656 [39] B. Mulloy, J. Hogwood, E. Gray, Assays and reference materials for current and future
657 applications of heparins, *Biologicals*, 38 (2010) 459-466.

658 [40] S. Bertini, A. Bisio, G. Torri, D. Bensi, M. Terbojevich, Molecular weight determination of heparin
659 and dermatan sulfate by size exclusion chromatography with a triple detector array,
660 *Biomacromolecules*, 6 (2005) 168-173.

661 [41] K. Jinno, Detection Principles., in: J. Cazes (Ed.) *Encyclopedia of Chromatography*, Third Edition
662 CRC Press2009, pp. 588-592.

- 663 [42] J.D. Mikkelsen, Purification of Betaine Aldehyde Dehydrogenase by Hydrophobic Interaction and
664 Affinity Column Chromatography, *J Cell Biochem*, (1987) 182-182.
- 665 [43] H. Ukeda, T. Ishii, M. Sawamura, H. Kusunose, Dynamic Analysis of the Binding Process of Bovine
666 Serum-Albumin on Glutaraldehyde-Activated Controlled-Pore Glass, *Anal Chim Acta*, 308 (1995) 261-
667 268.
- 668 [44] P. Halevi, R. Del Sole, in *Photonic Probes of Surfaces*, in: Elsevier (Ed.)Amsterdam, 1995, pp. 131.
- 669 [45] D.A. Lane, G. Pejler, A.M. Flynn, E.A. Thompson, U. Lindahl, Neutralization of heparin-related
670 saccharides by histidine-rich glycoprotein and platelet factor 4, *J Biol Chem*, 261 (1986) 3980-3986.
- 671 [46] S. Middeldorp, Heparin: from animal organ extract to designer drug, *Thromb Res*, 122 (2008)
672 753-762.
- 673 [47] J.F.W. Keuren, S.J.H. Wielders, A. Driessen, M. Verhoeven, M. Hendriks, T. Lindhout, Covalently-
674 bound heparin makes collagen thromboresistant, *Arterioscl Throm Vas*, 24 (2004) 613-617.
- 675 [48] T. Lindhout, R. Blezer, P. Schoen, G.M. Willems, B. Fouache, M. Verhoeven, M. Hendriks, L.
676 Cahalan, P.T. Cahalan, Antithrombin activity of surface-bound heparin studied under flow conditions,
677 *J Biomed Mater Res*, 29 (1995) 1255-1266.
- 678 [49] C. Arnander, P. Olsson, O. Larm, Influence of blood flow and the effect of protamine on the
679 thromboresistant properties of a covalently bonded heparin surface, *J Biomed Mater Res*, 22 (1988)
680 859-868.
- 681 [50] K. Kodama, B. Pasche, P. Olsson, J. Swedenborg, L. Adolfsson, O. Larm, J. Riesenfeld,
682 Antithrombin III binding to surface immobilized heparin and its relation to F Xa inhibition, *Thromb*
683 *Haemost*, 58 (1987) 1064-1067.
- 684 [51] B. Pasche, K. Kodama, O. Larm, P. Olsson, J. Swedenborg, Thrombin inactivation on surfaces
685 with covalently bonded heparin, *Thromb Res*, 44 (1986) 739-748.
- 686 [52] J. Maia, R.A. Carvalho, J.F.J. Coelho, P.N. Simões, M.H. Gil, Insight on the periodate oxidation of
687 dextran and its structural vicissitudes, *Polymer*, 52 (2011) 258-265.
- 688 [53] M.F. Ishak, T.J. Painter, Kinetic evidence for hemiacetal formation during the oxidation of
689 dextran in aqueous periodate, *Carbohydrate Research*, 64 (1978) 189-197.
- 690 [54] S. Gore, J. Andersson, R. Biran, C. Underwood, J. Riesenfeld, Heparin surfaces: Impact of
691 immobilization chemistry on hemocompatibility and protein adsorption, *Journal of biomedical*
692 *materials research. Part B, Applied biomaterials*, 102 (2014) 1817-1824.
- 693 [55] S.T. Baksaas, V. Videm, T. Pedersen, H. Karlsen, T.E. Mollnes, F. Brosstad, J.L. Svennevig,
694 Comparison of three oxygenator-coated and one total-circuit-coated extracorporeal devices,
695 *Perfusion*, 14 (1999) 119-127.
- 696 [56] D.Y. Lee, Z. Khatun, J.-H. Lee, Y.-k. Lee, I. In, Blood Compatible Graphene/Heparin Conjugate
697 through Noncovalent Chemistry, *Biomacromolecules*, 12 (2011) 336-341.
- 698 [57] A. Dirksen, T.M. Hackeng, P.E. Dawson, Nucleophilic catalysis of oxime ligation, *Angew Chem Int*
699 *Ed Engl*, 45 (2006) 7581-7584.
- 700 [58] S.E. Sakiyama-Elbert, Incorporation of heparin into biomaterials, *Acta Biomater*, 10 (2014) 1581-
701 1587.
- 702 [59] K.O. Doh, Y. Yeo, Application of polysaccharides for surface modification of nanomedicines,
703 *Therapeutic delivery*, 3 (2012) 1447-1456.

704

705

706

707 **Figure Captions**

708 Figure 1. The heparin monomers typically consist of disaccharides that vary functionality (R-
709 group) by -H, SO₃, or acetyl groups—H and SO₃, have a specific method of cleavage that
710 can yield terminal aldehyde groups. i) Heparin is depolymerized by nitrous acid (HNO₂) to
711 form the heparin-aldehyde at the oligomer terminus position. ii) Aniline acetate reagent reacts
712 with the aldehyde to form the Schiff base iii) Sodium cyano-borohydride can be used to
713 reduce the Schiff-base to the phenylamine. GlcNSO₃ (N-sulfated-glucosamines), GlcN (N-
714 unsubstituted glucosamines), GlcNAc (N-acetylated-glucosamines).

715
716 Figure 2. Size exclusion chromatography of unfractionated heparin (black line) vs heparin
717 fractionated at pH 1.5 (dotted black line) and pH 4.0 (grey line) after 10 min incubation at
718 25°C. A) Differential refractive index detector and B) UV absorbance detector at 280 nm. C)
719 LEFT AXIS: UV absorbance detector at 369 nm comparing SEC profiles of heparin-aldehyde
720 (black line), heparin-Schiff base (grey line), and the reduced heparin phenylamine (black
721 dash). RIGHT AXIS: Refractive index spectra that is representative of the of a 100 µg
722 injection of optimized heparin-aldehyde.

723
724 Figure 3. A) Heparin depolymerization at pH 1.5 in nitrous acid, specifically targeting the
725 GlcNSO₃ containing disaccharides. Left axis: Weight-averaged molar mass (M_w , top of bar)
726 and number-averaged molar mass (M_n , bottom of bar) at two reaction temperatures, 0°C
727 (black bar) and 25°C (grey bar). Bar ‘lengths’ allow direct comparison of polydispersity
728 between formulations. M_w and M_n values are generally regarded to be accurate within ±10%.
729 Right axis: Molar ratio of heparin disaccharides (570 Da) to aldehydes at two reaction
730 temperatures, 0°C (black square) and 25°C (grey square). Aldehyde ratios were quantified by
731 UV/Vis absorption ($\lambda = 369$ nm) of their corresponding aniline Schiff-bases. B) Heparin
732 depolymerization at pH 4.0 in nitric acid, specifically targeting the GlcN containing
733 disaccharides. C) Percent reaction yield of oligosaccharides after nitric acid depolymerization
734 and dialysis fractionation using 10 kDa molecular-weight cut-off tubing.

735 Figure 4. Above) Reaction scheme of PCL strips surface functionalized with optimized
736 heparin-aldehyde, PCL-HEP, through the intermediate, PCL-NH₂. Below) PCL-NH₂ and
737 PCL-HEP samples analyzed by XPS with spectra peaks displayed for C1s, O1s, N1s, and S2p
738 and their decomposition. XPS data is summarized in Table 2.

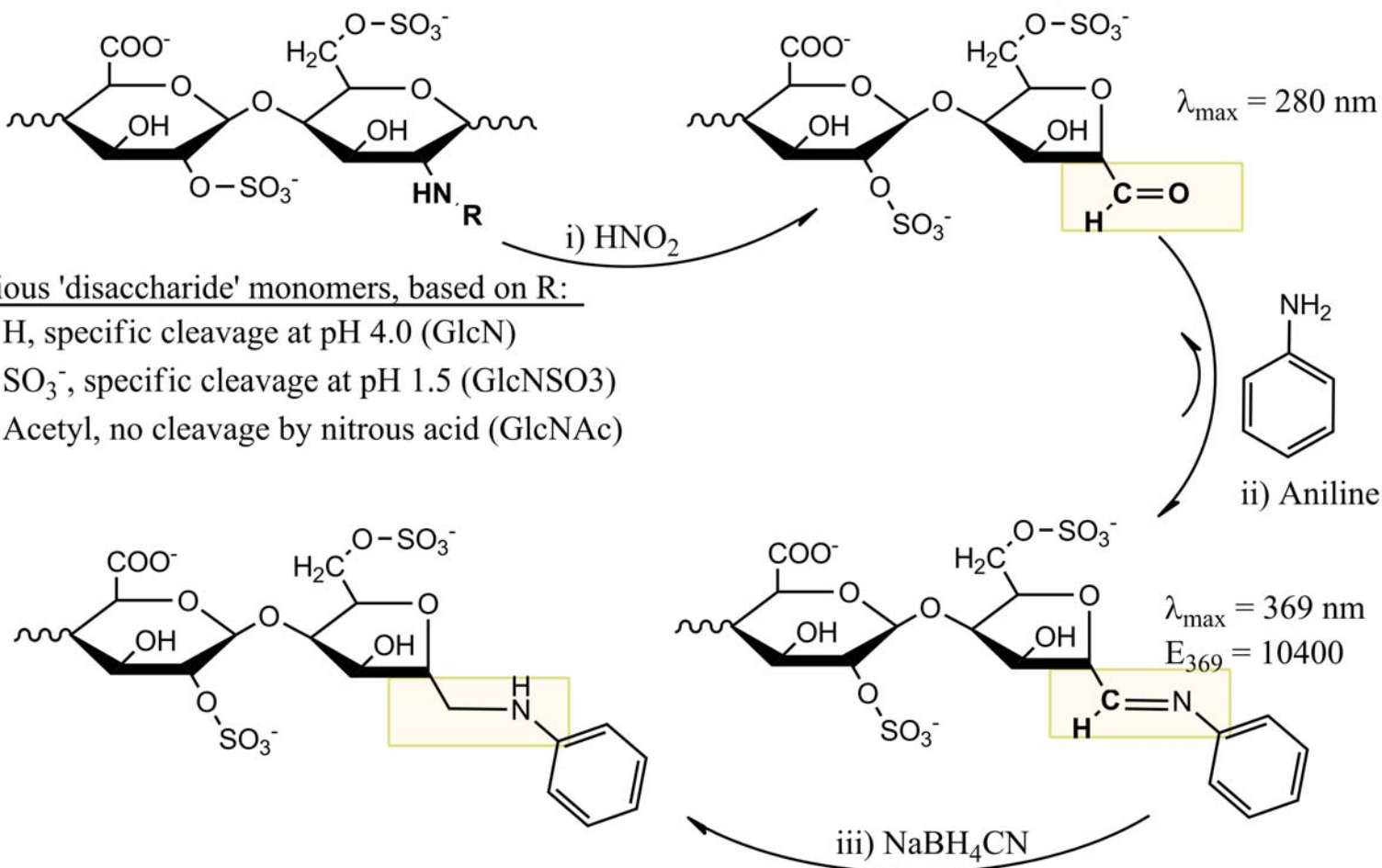
739 Figure 5. A) Heparin Aldehyde anticoagulant properties quantitatively by colorimetric
740 analysis at 540nm of released hemoglobin from non-clotted erythrocytes in recalcified
741 citrated blood across a time course and qualitatively, the side image shows a comparison of
742 blood clotting in the presence of BOTTOM: PBS buffer ‘No Heparin’ (control), MIDDLE:
743 unmodified and unfractionated “heparin”, and RIGHT: optimized “heparin-aldehyde”. Size
744 of blood clot formed after 1 h incubation is estimated through clot surface area percentage
745 with respect to total petri dish area. B) Time course for coagulation of recalcified citrated
746 blood on PCL films with and without heparin treatments also by the colorimetric detection of
747 non clotted erythrocyte hemoglobin. C) Thrombosis formation on PCL films. PCL,
748 polycaprolactone film with no surface modifications was used as reference with a normalized
749 value of 1. PCL-MPH, surface functionalized PCL strips with covalently bound unmodified
750 heparin. PCL-AHA, optimized heparin-aldehyde (electrostatically bound) on PCL. PCL-
751 HEP, covalently crosslinked optimized heparin-aldehyde, terminal aldehyde attachment,
752 through Schiff base reduction. Significant differences compared with PCL and PCL-MPH
753 against PCL-AHA and PCL-HEP. D) Surface chemistry of pristine PCL, PCL-MPH, PCL-
754 AHA, and PCL-HEP.

755 Figure 6. A) Platelet adhesion on heparin-modified PCL relative to pristine PCL. PCL,
756 pristine polycaprolactone, unmodified. PCL-AHA, optimized heparin-aldehyde
757 (electrostatically bound) on PCL. PCL-HEP, covalently crosslinked optimized heparin-
758 aldehyde, terminal aldehyde attachment, through Schiff base reduction. Significant
759 differences compared with PCL. B) Representative SEM images of PCL and heparin-
760 modified PCL strips after incubation with platelet-rich plasma.

761 Graphical Abstract Caption: Size exclusion chromatography protocol facilitates assay
762 development by detection of aldehydes and Schiff base functional groups found on
763 macromolecules in both aqueous and organic solvents. Online analysis with light scattering,
764 refractive index and UV detectors allows molar mass, concentrations of polymer and
765 aldehyde containing analytes to be quantified independently and simultaneously, with
766 heparin-aldehyde employed as a model molecule for development.

L-iduronate-2-sulfate, N-sulfo-D-glucosamine-6-sulfate
(R=SO₃⁻) heparin disaccharide monomer

Figure 1



Various 'disaccharide' monomers, based on R:

R = H, specific cleavage at pH 4.0 (GlcN)

R = SO₃⁻, specific cleavage at pH 1.5 (GlcNSO₃)

R = Acetyl, no cleavage by nitrous acid (GlcNAc)

Figure 2

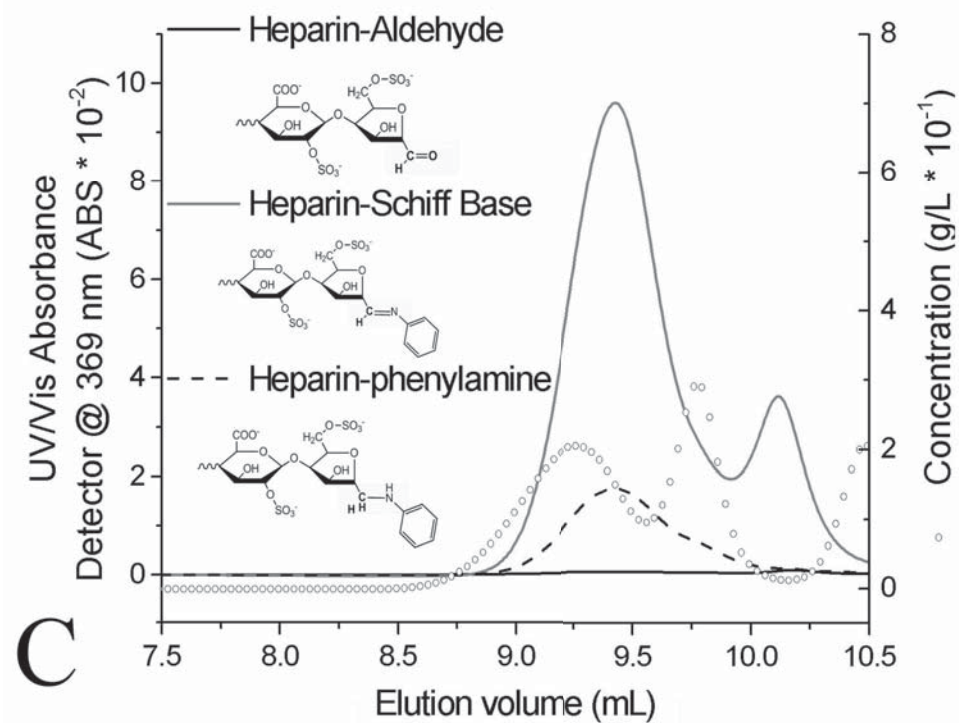
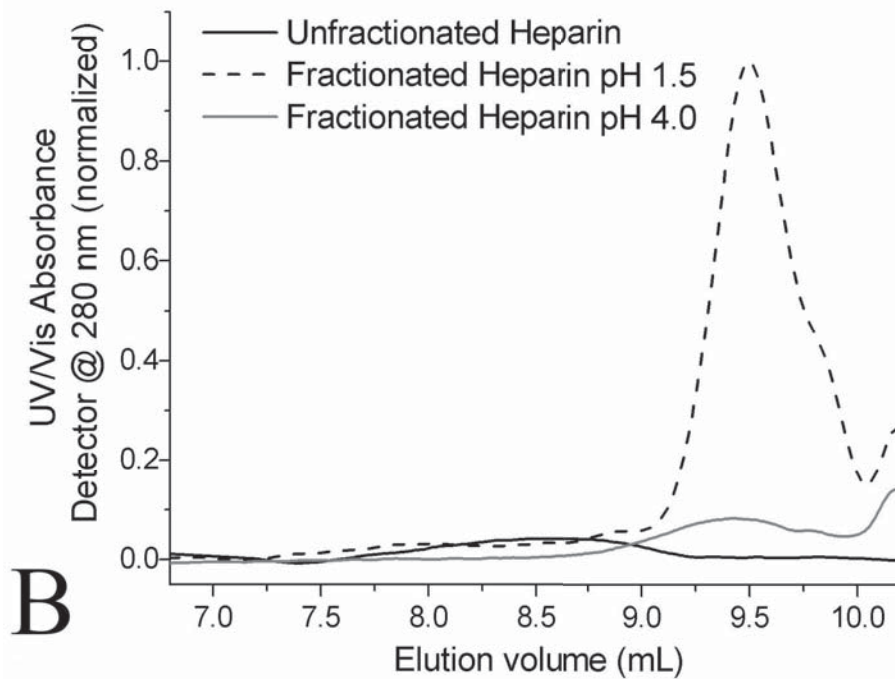
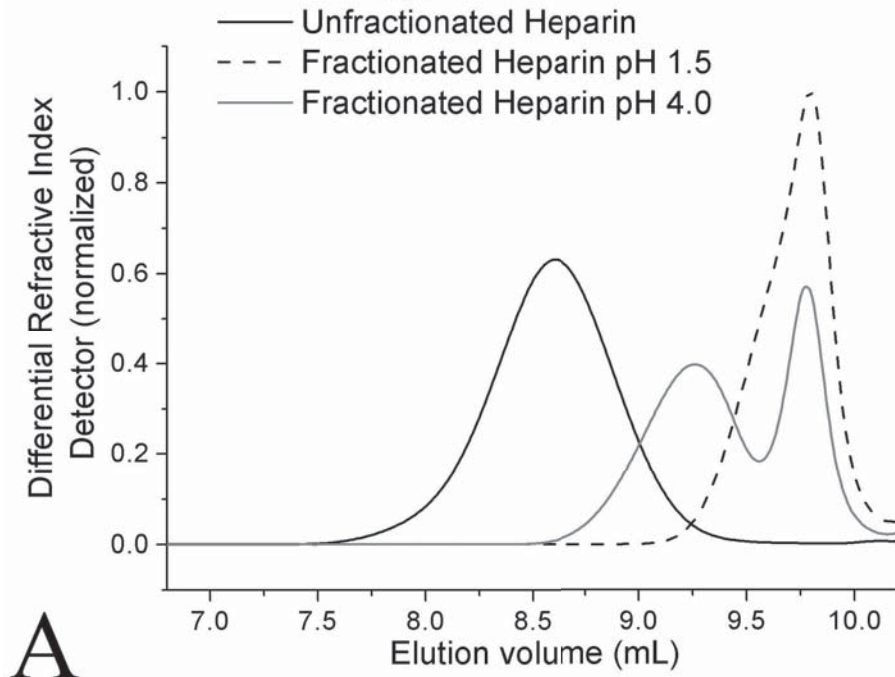


Figure 3

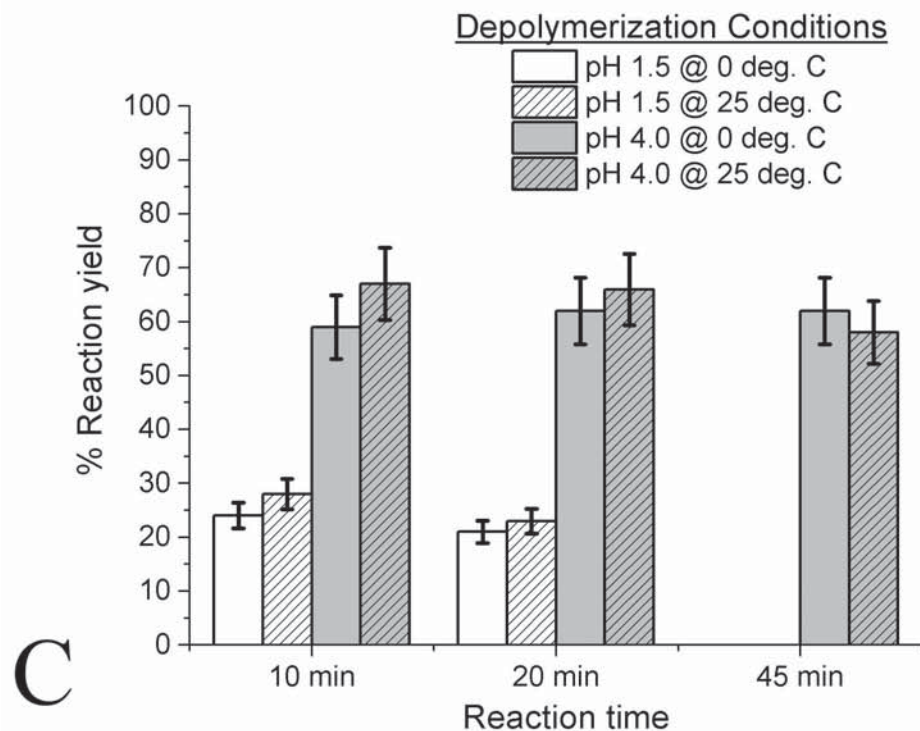
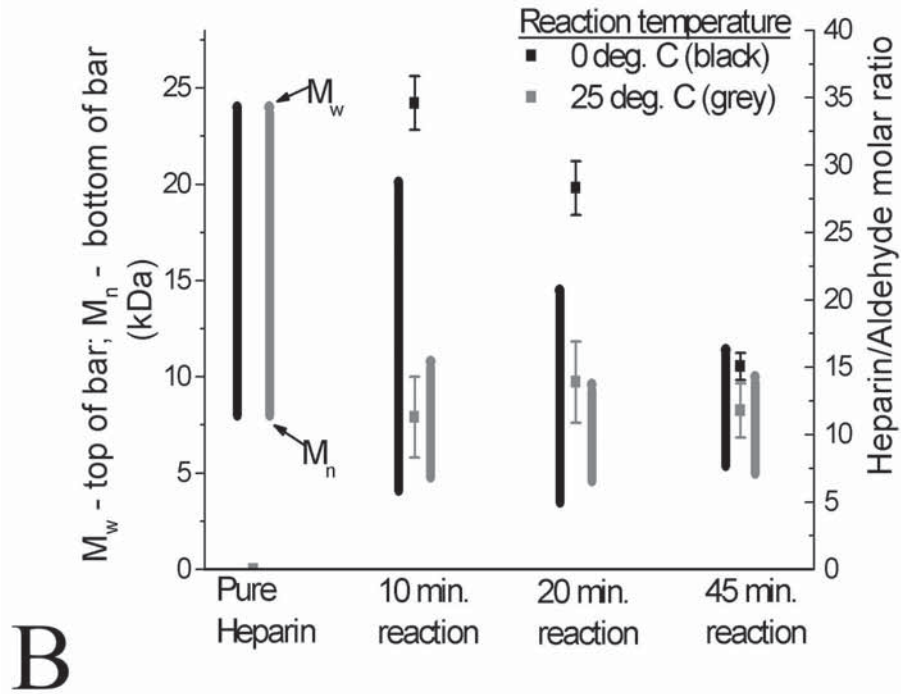
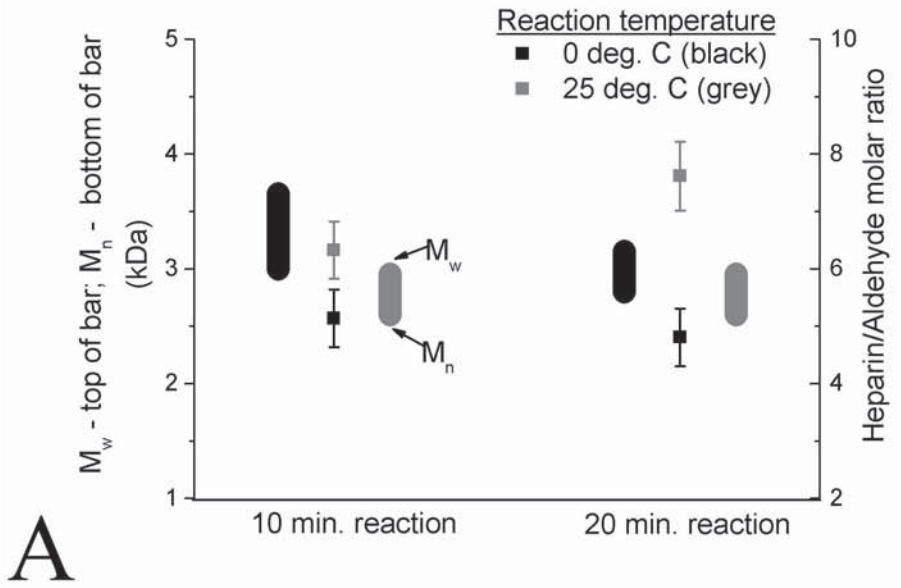
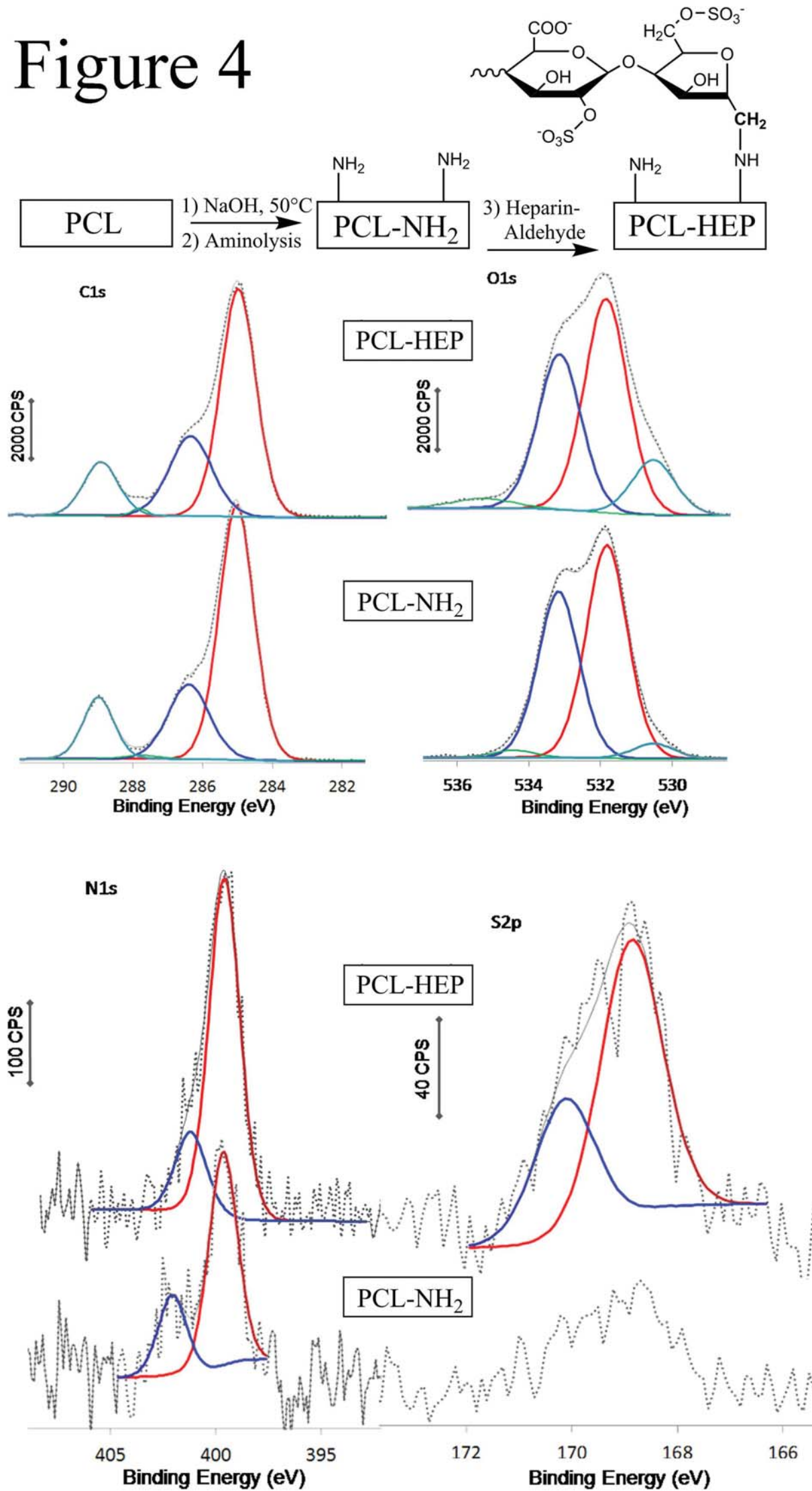
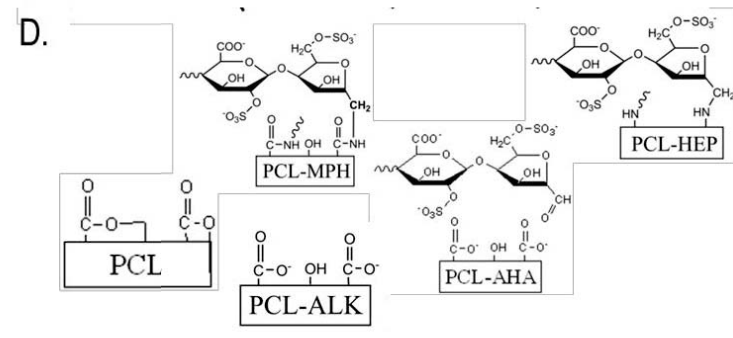
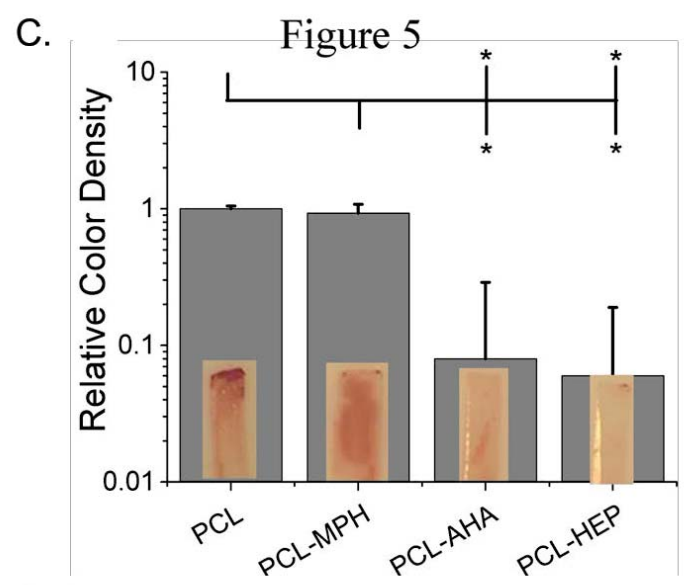
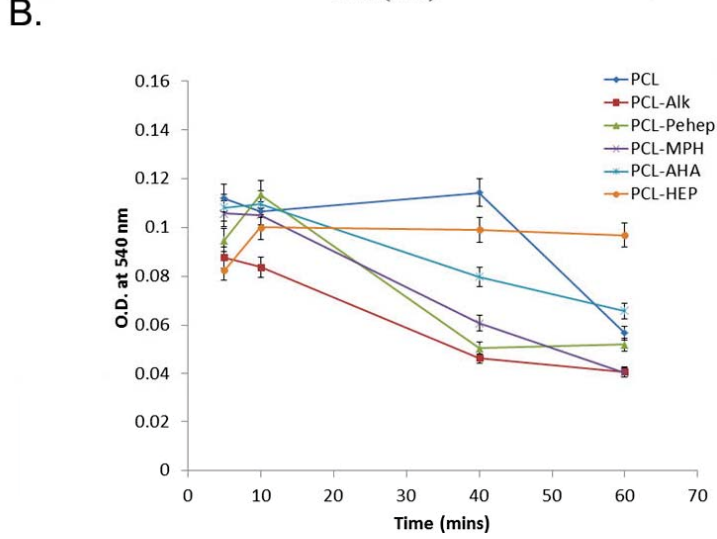
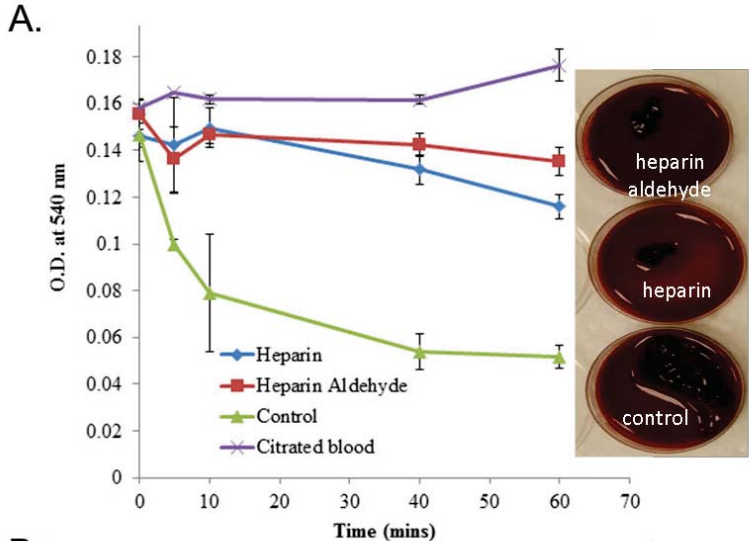


Figure 4





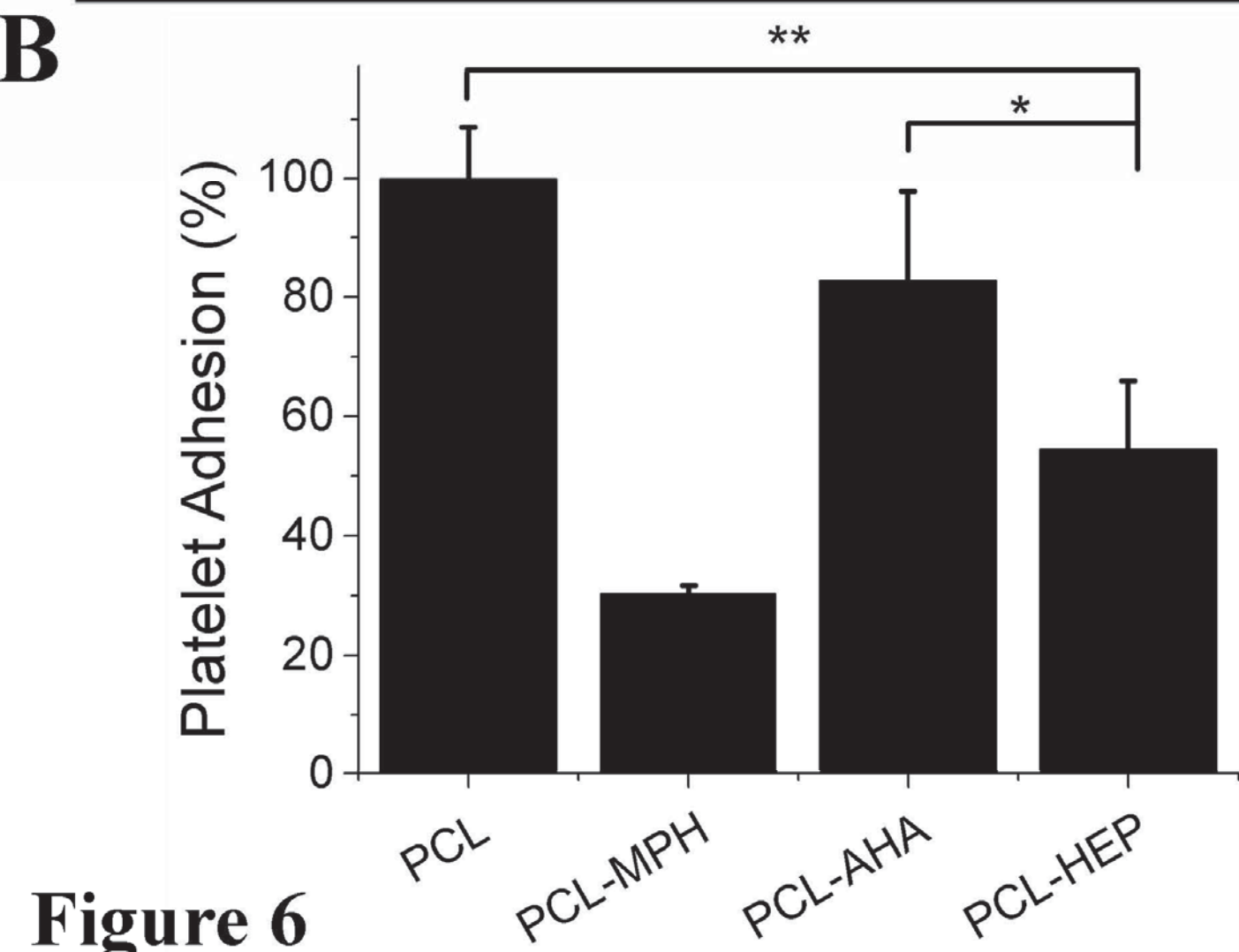
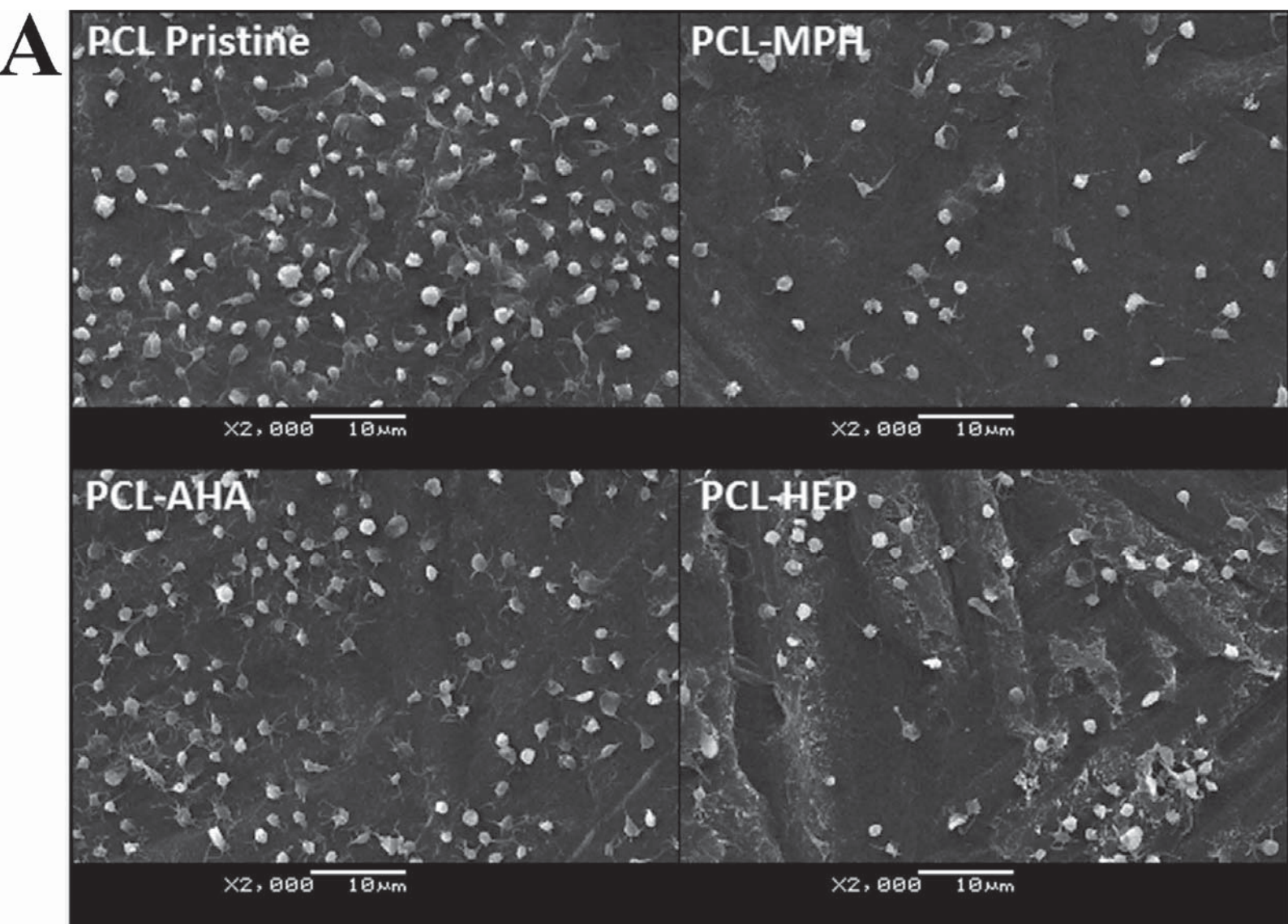
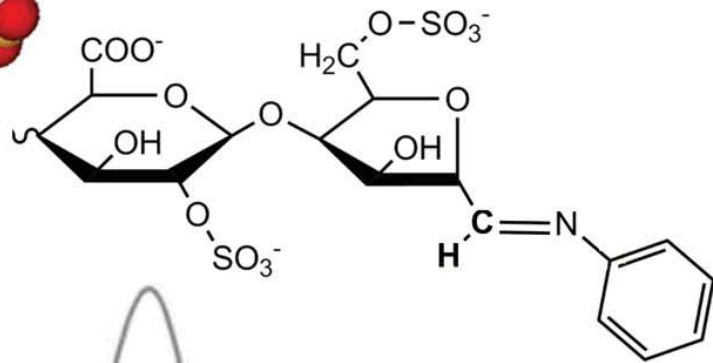
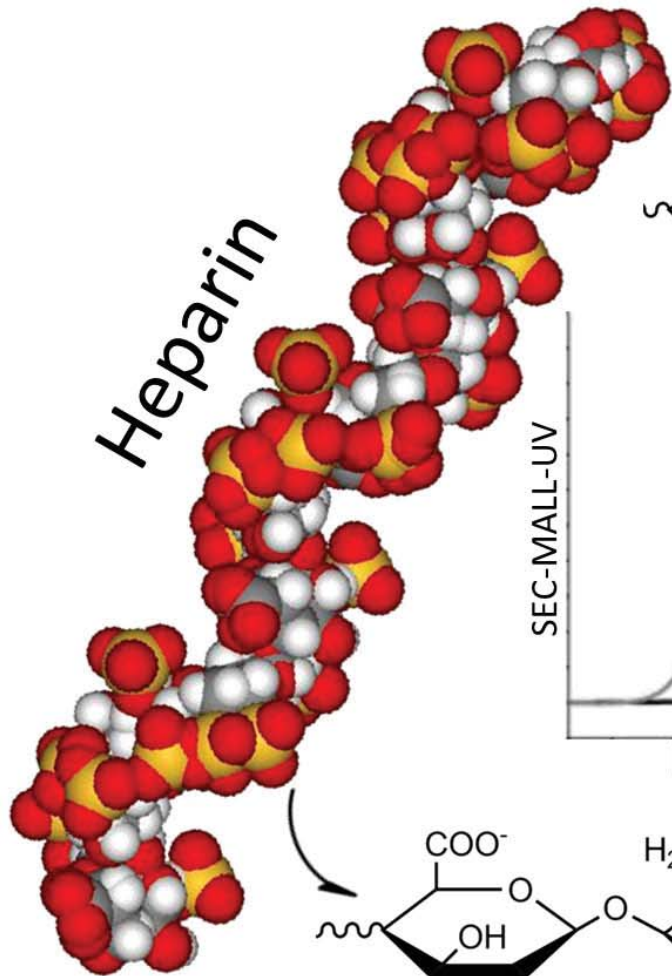
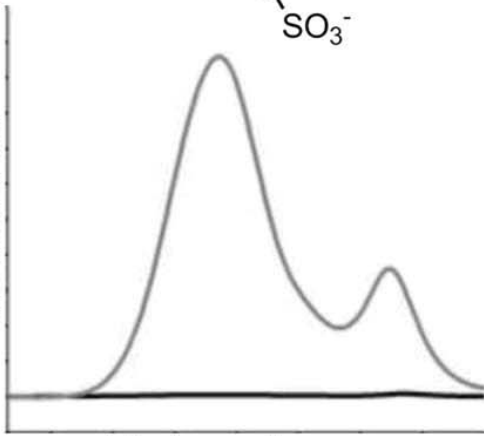


Figure 6

Heparin



SEC-MALL-UV



Elution volume

